Phase Transitions of the Flux Line Lattice in High-Temperature Superconductors with Weak Columnar and Point Disorder

Yadin Y. Goldschmidt

Department of Physics and Astronomy

University of Pittsburgh

Pittsburgh, PA 15260

(March 9, 1997)

arXiv:cond-mat/9703166v1 17 Mar 1997

Abstract

We study the effects of weak point and columnar disorder on the vortex-lattice phase transitions in high temperature superconductors. The combined effect of thermal fluctuations and of quenched disorder is investigated using a simplified cage model. For point disorder we use the mapping to a directed polymer in a disordered medium in 2+1 dimensions. For columnar disorder the problem is mapped into a quantum particle in a harmonic + random potential. We use the variational approximation to show that point and columnar disorder have opposite effect on the position of the melting line as is observed experimentally. For point disorder, replica symmetry breaking plays a role at the transition into a vortex glass at low temperatures.

74.60.Ec,74.60.Ge

Typeset using REVTEX

I. INTRODUCTION

There is a lot of interest in the physics of high temperature superconductors due to their potential technological applications. In particular these materials are of type II and allow for partial magnetic flux penetration. Pinning of the magnetic flux lines (FL) by many types of disorder is essential to eliminate dissipative losses associated with flux motion. In clean materials below the superconducting temperature there exist a 'solid ' phase where the vortex lines form a triangular Abrikosov lattice [1]. In the presence of impurities it was suggested [2] the Abrikosov crystal is replaced by a dislocation -free 'Bragg glass' which is also characterized by (quasi-) long range order. This 'solid' can melt due to thermal fluctuations or changes in the magnetic field. In particular known observed transitions are into a flux liquid at higher temperatures via a first-order *melting line* (ML) [3], and into a vortex glass at low temperature [4], [5], in the presence of disorder- the so called *entanglement line* (EL). [1]

Recently the effect of point and columnar disorder on the position of the melting transition has been measured experimentally in the high-T_c material $Bi_2Sr_2CaCu_2O_8$ [6](BSCCO). Point disorder has been induced by electron irradiation (with 2.5 MeV electrons), whereas columnar disorder has been induced by heavy ion irradiation (1 GeV Xe or 0.9 GeV Pb). It turns out that the flux melting transition persists in the presence of either type of disorder, but its position shifts depending on the disorder type and strength.

A significant difference has been observed between the effects of columnar and point disorder on the location of the ML. Weak columnar defects stabilize the solid phase with respect to the vortex liquid phase and shift the transition to *higher* fields, whereas point-like disorder destabilizes the vortex lattice and shifts the melting transition to *lower* fields. In this paper we attempt to provide a quantitative explanation to this observation. The case of point defects has been addressed in a recent paper by Ertas and Nelson [7] using the cage-model approach which replaces the effect of vortex-vortex interactions by an harmonic potential felt by a single vortex. For columnar disorder the parabolic cage model was introduced

by Nelson and Vinokur [8]. Here we use an analytic approach to analyze the cage-model Hamiltonian vis. the replica method together with the variational approximation. In the case of columnar defects our approach relies on our recent analysis of a quantum particle in a random potential [9,10]. We compare the effect of the two types of disorder with each other and with results of recent experiments.

Assume that the average magnetic field is aligned along the z-axis which is also the c-axis of BSCCO, i.e. perpendicular to the CuO planes. Following EN we describe the Hamiltonian of a single FL whose position is given by a two-component vector $\mathbf{r}(z)$ (overhangs are neglected) by:

$$\mathcal{H} = \int_0^L dz \left\{ \frac{\epsilon_l}{2} \left(\frac{d\mathbf{r}}{dz} \right)^2 + V(z, \mathbf{r}) + \frac{\mu}{2} \mathbf{r}^2 \right\}. \tag{1.1}$$

Here $\epsilon_l = \epsilon_0/\gamma^2$ is the line tension of the FL, $\gamma^2 = m_z/m_\perp$ is the mass anisotropy, $\epsilon_0 = (\Phi_0/4\pi\lambda)^2$, (Φ_0 is the fluxoid and λ is the penetration length), and $\mu \approx \epsilon_0/a_0^2$ is the effective spring constant (setting the cage size) due to interactions with neighboring FLs, which are at a typical distance of $a_0 = \sqrt{\Phi_0/B}$ apart.

For the case of point-disorder, V depends on z and [7]

$$\langle V(z, \mathbf{r}) V(z', \mathbf{r}') \rangle = \tilde{\Delta} \epsilon_0^2 \xi^3 \delta_\xi^{(2)}(\mathbf{r} - \mathbf{r}') \delta(z - z'). \tag{1.2}$$

where

$$\delta_\xi^{(2)}(\mathbf{r} - \mathbf{r}') \approx 1/(2\pi\xi^2) \exp(-(\mathbf{r} - \mathbf{r}')^2/2\xi^2), \tag{1.3}$$

and ξ is the vortex core diameter. The dimensionless parameter $\tilde{\Delta}$ is a measure of the strength of the disorder. In this case the Hamiltonian is exactly the same as that of a directed polymer in a random medium in 2+1 dimensions [11]. The vortex line represents the polymer which is directed along the z-axis (overhangs are neglected). The presence of impurities enhances the transverse wandering of the polymer.

For the case of columnar (or correlated) disorder, $V(z, \mathbf{r}) = V(\mathbf{r})$ is independent of z, and

$$\langle V(\mathbf{r})V(\mathbf{r}')\rangle \equiv -2f((\mathbf{r}-\mathbf{r}')^2/2) = g\epsilon_0^2\xi^2\delta_\xi^{(2)}(\mathbf{r}-\mathbf{r}'), \tag{1.4}$$

In this case we map the problem of a FL in a superconductor into that of a quantum particle in a random potential. The partition function of the quantum particle is just like the partition sum of the FL, provided one make the identification [8]

$$\hbar \to T, \qquad \beta\hbar \to L, \tag{1.5}$$

Where T is the temperature of the superconductor and L is the system size in the z-direction. β is the inverse temperature of the quantum particle. We are interested in large fixed L as T is varied, which corresponds to high β for the quantum particle when $\hbar$ (or alternatively the mass of the particle) is varied. The variable z is the so called Trotter time.

The quantity which measures the transverse excursion of the FL is

$$u_0^2(\ell) \equiv \langle |\mathbf{r}(z) - \mathbf{r}(z+\ell)|^2\rangle /2, \tag{1.6}$$

The main effect of the harmonic (or cage) potential is to cap the transverse excursions of the FL beyond a confinement length $\ell^* \approx a_0/\gamma$. This length arises by equating the elastic energy and the cage potential energy of the FL. Typically after it wanders a distance ℓ^* along the z-direction the FL is reflected back by the walls of the cage and restarts its transverse excursions. The near saturation of $u_0^2(\ell)$ at $\ell = \ell^*$ will become evident from the analytical expressions derived in the following sections. We thus define the mean square displacement of the flux line by

$$u^2(T) = u_0^2(\ell^*). \tag{1.7}$$

The location of the melting line is determined by the Lindemann criterion

$$u^2(T_m(B)) = c_L^2 a_0^2, \tag{1.8}$$

where $c_L \approx 0.15 - 0.2$ is the phenomenological Lindemann constant. This means that when the transverse excursion of a section of length $\approx \ell^*$becomes comparable to a finite fraction of the interline separation a_0, the melting of the flux solid occurs.

II. THE CASE OF POINT DISORDER

We start with the case of point disorder that is simpler mathematically. In this case, the problem is equivalent to a directed polymer in a combination of a random potential and a fixed harmonic potential. The flux line plays the role of the polymer directed along the z-axis. The cage potential supplies the harmonic part of the potential and the defects, or impurities, the random part. The problem of directed polymers has been investigated extensively in the literature in the absence of the harmonic piece. Here we follow the approach of Mezard and Parisi (MP) [11], who used the so called variational (or Hartree) approximation. They set up the problem in the presence of a harmonic piece with spring constant μ, but they were mainly concerned with the limit of $\mu \to 0$.

Recall that the Hamiltonian $\mathcal{H}$ representing the system is given (within the framework of the cage model) by eq. (1.1), together with probability distribution for the random potential whose second moment is given by:

$$\langle V(z,\mathbf{r})V(z',\mathbf{r}')\rangle = \tilde{\Delta}\epsilon_0^2\xi^3\delta_\xi^{(2)}(\mathbf{r}-\mathbf{r}')\delta(z-z'). \tag{2.1}$$

In order to average over the quenched random potential, the replica method is used. After introducing n copies of the fields and averaging over the potential one obtains:

$$\langle Z^n\rangle = \int d[\mathbf{r}_1]\dots d[\mathbf{r}_n]\ exp(-\beta H_n)\ , \tag{2.2}$$

with the replicated n-body Hamiltonian given by:

$$H_n = \frac{\epsilon_l}{2}\int_0^L dz \sum_{a=1}^n \left(\frac{d\mathbf{r}_a}{dz}\right)^2 + \frac{\mu}{2}\int dz\ \sum_{a=1}^n (\mathbf{r}_a(z))^2 - \frac{\beta}{2}\frac{\tilde{\Delta}}{2\pi}\xi\epsilon_0^2\int dz\ \sum_{a,b}\exp(-\frac{(\mathbf{r}_a-\mathbf{r}_b)^2}{2\xi^2})\ , \tag{2.3}$$

The variational quadratic Hamiltonian associated with the replica Hamiltonian H_n is parametrized by:

$$h_n = \frac{1}{2}\int_0^L dz \sum_a [\epsilon_l\ \dot{\mathbf{r}}_a^2 + \mu\mathbf{r}_a^2] - \frac{1}{2}\int_0^L dz \sum_{a,b} s_{ab}\ \mathbf{r}_a(z)\cdot\mathbf{r}_b(z), \tag{2.4}$$

where s_{ab} is the $n \times n$ matrix of parameters needed to be determined by the variational principles.

These parameters are fixed by extremizing the variational free-energy given by:

$$F = \langle H_n - h_n \rangle_{h_n} - \frac{1}{\beta} \ln \left(\int d[\mathbf{r}_a] \ \exp(-\beta h_n) \right). \tag{2.5}$$

This free energy is given by:

$$\begin{aligned} \frac{F}{2L} &= \frac{1}{2\beta} \sum_{ab} s_{ab} \int_{-\infty}^{\infty} \frac{d\omega}{2\pi} G_{ab}(\omega) - \frac{1}{2\beta} \int \frac{d\omega}{2\pi} \mathrm{Tr} \ln G(\omega) \\ &- \frac{\beta}{4} \frac{\tilde{\Delta}}{2\pi} \xi \epsilon_0^2 \sum_{a,b} \sum_{m=0}^{\infty} \frac{(-)^m}{2^m \xi^{2m} m!} \left\langle (\mathbf{r}_a(z) - \mathbf{r}_b(z))^{2m} \right\rangle_{h_n}, \end{aligned} \tag{2.6}$$

where $G(\omega)$ is the propagator associated with h_n :

$$[G^{-1}(\omega)]_{ab} = (\epsilon_l \ \omega^2 + \mu)\delta_{ab} - s_{ab}, \tag{2.7}$$

and ω is the 'momentum' variable conjugate to z. Since we are interested in the limit $L \to \infty$ we can assume that ω is a continuous variable. Using the formula (for a two dimensional vector field $\mathbf{r}$):

$$\left\langle (\mathbf{r}_a(z) - \mathbf{r}_b(z))^{2m} \right\rangle_{h_n} = \frac{2^m m!}{\beta^m} \left(\int \frac{d\omega}{2\pi} [G_{aa}(\omega) + G_{bb}(\omega) - 2G_{ab}(\omega)] \right)^m, \tag{2.8}$$

we finally arrive at the result:

$$\begin{aligned} \frac{F}{2L} &= const. + \frac{1}{2\beta} \int \frac{d\omega}{2\pi} (\epsilon_l \ \omega^2 + \mu) \sum_a G_{aa}(\omega) - \frac{1}{2\beta} \int \frac{d\omega}{2\pi} \mathrm{Tr} \ln G(\omega) \\ &+ \frac{\beta}{2} \sum_{ab} \widehat{f}_p\left(\frac{1}{\beta} \int \frac{d\omega}{2\pi} [G_{aa}(\omega) + G_{bb}(\omega) - 2G_{ab}(\omega)]\right), \end{aligned} \tag{2.9}$$

where the function $\widehat{f}_p$ is given by:

$$\widehat{f}_p(y) = -\frac{\widetilde{\Delta} \epsilon_0^2 \xi^3}{4\pi} \frac{1}{\xi^2 + y} \tag{2.10}$$

Stationarity of the free energy with respect to the parameters s_{ab} gives:

$$\begin{aligned} s_{ab} &= 2\beta \widehat{f}_p'\left(\frac{1}{\beta} \int \frac{d\omega}{2\pi} [G_{aa}(\omega) + G_{bb}(\omega) - 2G_{ab}(\omega)]\right), \quad a \neq b \\ s_{aa} &= - \sum_{b(\neq a)} s_{ab}. \end{aligned} \tag{2.11}$$

Here $\widehat{f}_p'$ is the derivative of $\widehat{f}_p(y)$ with respect to its argument.

We consider first the replica symmetric (RS) case, where all the off diagonal elements of s_{ab} are taken to be equal to each other and their value denoted by s. We denote the value of the diagonal elements by s_d. Eq.(2.11) implies that in the limit $n \to 0$, $s_d = s$.

In this limit we find:

$$G_{ab}(\omega) = \frac{\delta_{ab}}{\epsilon_l\ \omega^2 + \mu} + \frac{s}{(\epsilon_l\ \omega^2 + \mu)^2}, \tag{2.12}$$

$$s = \frac{2}{T}\widehat{f}_p\ '(\tau). \tag{2.13}$$

Here we introduced the reduced temperature variable

$$\tau = T/\sqrt{\epsilon_l \mu}. \tag{2.14}$$

Using these results we can calculate the mean square displacement (1.6):

$$\begin{aligned} u_0^2(\ell) &= \frac{2}{\beta}\int \frac{d\omega}{2\pi}(1-\cos(\omega\ell))G_{aa}(\omega) \\ &= 2T\int \frac{d\omega}{2\pi}\frac{1-\cos(\omega\ell)}{\epsilon_l\ \omega^2+\mu}(1+\frac{s}{\epsilon_l\ \omega^2+\mu}), \end{aligned} \tag{2.15}$$

and hence

$$\begin{aligned} u_0^2(\ell) = \tau(1-e^{-\ell/\ell^*}) + \tau\ s\ /\ (2\mu) \\ \times\ (1-e^{-\ell/\ell^*} - (\ell/\ell^*)\ e^{-\ell/\ell^*}), \end{aligned} \tag{2.16}$$

with

$$s = \frac{\epsilon_0^2\xi^3}{T}\frac{\widetilde{\Delta}}{2\pi}\frac{1}{(\xi^2+\tau)^2}, \quad \ell^* = \sqrt{\epsilon_l/\mu}. \tag{2.17}$$

Note that s is positive and independent of ω, and hence the mean square displacement $u_0^2(\ell^*)$ is bigger than its value for zero disorder.

At this point it is convenient to introduce dimensionless variables:

$$\widetilde{T} = T/(\epsilon_0\xi), \tag{2.18}$$

$$\widetilde{B} = B\xi^2/\Phi_0. \tag{2.19}$$

In terms of these variables

$$\mu = \widetilde{B}\ \epsilon_0/\xi^2, \quad a_0^2 = \xi^2/\widetilde{B}, \tag{2.20}$$

$$\tau = \xi^2\gamma\widetilde{T}\ /\ \sqrt{\widetilde{B}}. \tag{2.21}$$

As parameters for BSCCO we take mean values for those quoted in ref. [1]:

$$\begin{aligned} \xi &\cong 30\mathring{A}, \\ \epsilon_0\xi &\cong 1905K,\ \text{(corresp. to } \lambda_L \approx 1700\mathring{A}) \\ \gamma &\cong 125. \end{aligned} \tag{2.22}$$

and also $\Phi_0 = 2.07 \times 10^{-7}$ G cm^2. In the case of the experiments one has

$$\widetilde{B} \ll (\gamma\widetilde{T})^2, \tag{2.23}$$

and hence:

$$u^2(T)\ /\ a_0^2 \simeq \sqrt{\widetilde{B}}\gamma\widetilde{T}\ (\ 1 - e^{-1}) + \frac{1}{2}\sqrt{\widetilde{B}}\left(\frac{\gamma\widetilde{\Delta}}{2\pi}\right)\frac{1}{(\gamma\widetilde{T})^2}\ (1 - 2e^{-1}) \tag{2.24}$$

Fig. 1 curve a shows a plot of $\sqrt{u_0^2(\ell^*)}/a_0$ vs. T for $\widetilde{\Delta}/2\pi = 0$ (curve a) and for $\widetilde{\Delta}/2\pi = 0.2$ (curve b). The value of the magnetic field is taken to be $B = 250G$.

Using the Lindemann criterion, eq. (1.8), we can easily solve for the magnetic field at the melting transition:

$$\widetilde{B}_m(\widetilde{T}) = c_L^4 \times \left(\gamma\widetilde{T}\ (\ 1 - e^{-1}) + \frac{1}{2}\left(\frac{\gamma\widetilde{\Delta}}{2\pi}\right)\frac{1}{(\gamma\widetilde{T})^2}\ (1 - 2e^{-1})\right)^{-2} \tag{2.25}$$

For $T < T_{cp}$ with

$$T_{cp} \approx (\epsilon_0\xi/\gamma)(\gamma\widetilde{\Delta}/2\pi)^{1/3} \tag{2.26}$$

it is necessary to break replica symmetry. This means that the off-diagonal elements of the variational matrix s_{ab} are not all equal to each other. MP [11] worked out the equations for the replica symmetry breaking (RSB) solution in the limit of $\mu \to 0$, but it is not difficult

to extend them to any value of μ. Their final solution is not applicable for the particular correlation $\widetilde{f}_p$ discussed in this paper, hence we will work it out below and in the Appendix.

When breaking replica symmetry *a la* Parisi, it is customary to introduce Parisi's parameter which is denoted here by u. Thus we put

$$s_{aa} = s_d, \tag{2.27}$$

$$a \neq b, \quad s_{ab} = s(u), \quad 0 \leq u \leq 1. \tag{2.28}$$

We have found that a 1-step RSB solution is sufficient in the present case and we parametrize it by:

$$s(u) = \begin{cases} s_0 & u < u_c \\ s_1 & u > u_c \end{cases} \tag{2.29}$$

$$\Sigma = u_c(s_1 - s_0). \tag{2.30}$$

In the following we will used the dimensionless variable $\widetilde{s} = s\xi^2/\epsilon_0$, and similarly for $\widetilde{\Sigma}$. In the case of the experiments, the assumption of small μ amounts to the condition (2.23) which is very well satisfied. For small μ we find (see Appendix for further details):

$$u_c = \widetilde{T}/\widetilde{T}_{cp}, \tag{2.31}$$

$$\widetilde{\Sigma} = (\gamma\widetilde{T}_{cp} - \gamma\widetilde{T})^2, \tag{2.32}$$

$$s_0 = \frac{1}{\gamma\widetilde{T}} \frac{\widetilde{B}}{(\gamma\widetilde{T}_{cp})^2} \left(\frac{\gamma\widetilde{\Delta}}{2\pi}\right), \tag{2.33}$$

$$\gamma\widetilde{T}_{cp} = \left(\frac{\gamma\widetilde{\Delta}}{2\pi}\right)^{1/3}. \tag{2.34}$$

Below T_{cp} the mean square displacement freezes at its value at T_{cp} :

$$u_0^2(T) \simeq u_0^2(T_{cp}), \quad T \leq T_{cp} \tag{2.35}$$

The 'freezing' temperature T_{cp} is about 1.33 larger than the temperature for which the RS expression for $u_0^2(T)$ (see equation (2.24) has a minimum. The value of the magnetic field corresponding to T_{cp} is $B_m(T_{cp}) \approx 2.07(\Phi_0/\xi^2)(\gamma\widetilde{\Delta}/2\pi)^{-2/3}c_L^4$ gives a reasonable agreement with the experiments as is evident from Figure 2.

In Figure 2 we show a plot of $B_m(T)$ vs. T for different values of the disorder. The points represent data reported by B. Khaykovitch *et al.* [6] for various amounts of point disorder (we also display points for columnar disorder as will be discussed in the next section). The theoretical fit is done using equation (2.25) for $T > T_{cp}$ and $B_m(T) = B_m(T_{cp})$, for $T < T_{cp}$. Best fit has been obtain by choosing $c_L = 0.162$ and $\widetilde{\Delta}/2\pi = 0.144$, 0.208 and 0.280 respectively. We have chosen the amount of disorder to best fit the temperature T_{cp} below which the experimental curves show an apparent change of behavior. This is achieved by using eq. (2.26). The fit associated with the value of $\widetilde{\Delta}/2\pi = 0.144$ is the one corresponding to the 'as grown' crystal which always has some amount of point defects. At high temperatures one observe somewhat larger deviations between the theoretical fits and the experimental data. This is due to the proximity to $T_c \approx 90K$, which affects the behavior of the melting line even for pure samples, see discussion in the concluding section. The flat part of the curves represent the so called *entanglement line*, which is believed to be a (continuous) transition into the vortex glass.

III. THE CASE OF COLUMNAR DISORDER

We consider first the case of columnar disorder. This problem maps into the problem of a quantum particle in a random potential. to see this we recall that the density matrix at finite temperature ($= \beta^{-1}$) of a quantum particle subject to a potential V is given by:

$$\rho(\mathbf{r}, \mathbf{r}', U) \;=\; \int_{\mathbf{r}(0)=\mathbf{r}}^{\mathbf{r}(U)=\mathbf{r}'} [d\mathbf{r}]\ \exp\left\{ -\frac{1}{\hbar} \int_0^U \left[\frac{m\dot{\mathbf{r}}(z)^2}{2} \;+\; \frac{\mu \mathbf{r}(z)^2}{2} \;+\; V(\mathbf{r}(z)) \right] dz \right\}, \qquad (3.1)$$

with $U = \beta\hbar$.The variable z has dimensions of time and is often referred to as the Trotter dimension. This is the same as the partition function of a single flux line, provided one makes the identification

$$\hbar \to T, \quad U = \beta\hbar \to L, \quad m \to \epsilon_l \qquad (3.2)$$

mentioned in the Introduction.

In the absence of disorder it is easily obtained from standard quantum mechanics and the correspondence (1.5), that when $L \to \infty$,

$$u^2(T) = \frac{T}{\sqrt{\epsilon_l \mu}} \left(1 - \exp(-\ell^* \sqrt{\mu/\epsilon_l})\right) = \frac{T}{\sqrt{\epsilon_l \mu}}(1 - e^{-1}), \tag{3.3}$$

When we turn on disorder we have to solve the problem of a quantum particle in a random quenched potential. This problem has been recently solved using the replica method and the variational approximation [9]. Let us review briefly the results of this approach. We apply the replica trick in order to carry out the quenched average over the random realizations. We consider n-copies of the system, and obtain for the averaged density matrix:

$$\rho(\mathbf{r}_1 \cdots \mathbf{r}_n, \mathbf{r}_1 \cdots \mathbf{r}_n, L) = \int_{\mathbf{r}_a(0)=\mathbf{r}_a}^{\mathbf{r}_a(L)=\mathbf{r}_a} \prod_{a=1}^{n} [d\mathbf{r}_a] \exp\{-\mathcal{H}_n/T\}, \tag{3.4}$$

$$\begin{aligned} \mathcal{H}_n &= \frac{1}{2}\int_0^L dz \sum_a \left[\epsilon_l \mathbf{r}_a^2(u) + \mu \mathbf{r}_a^2(u)\right] \\ &+ \frac{1}{2T}\int_0^L dz \int_0^L dz' \sum_{ab} 2\, f\left(\frac{(\mathbf{r}_a(z) - \mathbf{r}_b(z'))^2}{2}\right), \end{aligned} \tag{3.5}$$

with

$$f(y) = -\frac{g\epsilon_0^2}{4\pi} \exp(-\frac{y}{\xi^2}) \tag{3.6}$$

In this approximation we chose the best quadratic Hamiltonian parametrized by the matrix $s_{ab}(z - z')$:

$$\begin{aligned} h_n = \frac{1}{2}\int_0^L dz \sum_a [\epsilon_l \dot{\mathbf{r}}_a^2 + \mu \mathbf{r}_a^2] \\ - \frac{1}{2T}\int_0^L dz \int_0^L dz' \sum_{a,b} s_{ab}(z - z') \mathbf{r}_a(z) \cdot \mathbf{r}_b(z'). \end{aligned} \tag{3.7}$$

Here the replica index $a = 1 \ldots n$, and $n \to 0$ at the end of the calculation. Again, this Hamiltonian is determined by stationarity of the variational free energy which is given by

$$\langle F \rangle_R / T = \langle H_n - h_n \rangle_{h_n} - \ln \int [d\mathbf{r}] \exp(-h_n/T), \tag{3.8}$$

The off-diagonal elements of s_{ab} can consistently be taken to be independent of z, whereas the diagonal elements are z-dependent. It is more convenient to work in frequency space,

where ω is the frequency conjugate to z. $\omega_j = (2\pi/L)j$, with $j = 0, \pm 1, \pm 2, \ldots$. Assuming replica symmetry, which is valid only for part of the temperature range, we can denote the off-diagonal elements of $\widetilde{s}_{ab}(\omega) = (1/T)\int_0^L dz\ e^{i\omega z}\ s_{ab}(z)$, by $\widetilde{s}(\omega) = \widetilde{s}\delta_{\omega,0}$. Denoting the diagonal elements by $\widetilde{s}_d(\omega)$, the variational equations become:

$$\tilde{s} = 2\frac{L}{T}\widehat{f}_c\,'\left(\frac{2T}{\mu L} + \frac{2T}{L}\sum_{\omega'\neq 0}\frac{1}{\epsilon_l\ \omega'^{\,2} + \mu - \widetilde{s}_d(\omega')}\right) \tag{3.9}$$

$$\begin{aligned}\tilde{s}_d(\omega) = \tilde{s} - \frac{2}{T}\int_0^L d\zeta\ (1 - e^{i\omega\zeta}) \times \\ \widehat{f}_c\,'\left(\frac{2T}{L}\sum_{\omega'\neq 0}\ \frac{1 - e^{-i\omega'\varsigma}}{\epsilon_l\omega'^{\,2} + \mu - \widetilde{s}_d(\omega')}\right).\end{aligned} \tag{3.10}$$

here $\widehat{f}_c\,'(y)$ denotes the derivative of the "dressed" function $\widehat{f}_c(y)$ which is obtained in the variational scheme from the random potential's correlation function $f(y)$, and in our case is given by:

$$\widehat{f}_c(y) = -\frac{g\epsilon_0^2\xi^2}{4\pi}\frac{1}{\xi^2 + y} \tag{3.11}$$

The full equations, taking into account the possibility of replica-symmetry breaking are given in ref. [9]. In terms of the variational parameters the function $u_0^2(\ell)$ is given by

$$u_0^2(\ell) = \frac{2T}{L}\sum_{\omega'\neq 0}\frac{1 - \cos(\omega'\ell^*)}{\epsilon_l\omega'^{\,2} + \mu - \widetilde{s}_d(\omega')}. \tag{3.12}$$

This quantity has not been calculated in ref. [9]. There we calculated $\langle \mathbf{r}^2(0)\rangle$ which does not measure correlations along the z-direction.

In the limit $L \to \infty$ we were able to solve the equations analytically to leading order in g. In that limit eq. (3.10) becomes (for $\omega \neq 0$) :

$$\begin{aligned}\tilde{s}_d(\omega) = \frac{4}{\mu}\widehat{f}_c\,''(b_0) - \frac{2}{T}\int_0^\infty d\varsigma(1 - \cos(\omega\varsigma)) \\ \times(\widehat{f}_c\,'(C_0(\varsigma)) - \widehat{f}_c\,'(b_0)),\end{aligned} \tag{3.13}$$

with

$$C_0(\varsigma) = 2T\int_{-\infty}^{\infty}\frac{d\omega}{2\pi}\frac{1 - \cos(\omega\varsigma)}{\epsilon_l\omega^{\,2} + \mu - \widetilde{s}_d(\omega)}, \tag{3.14}$$

$$b_0 = 2T\int_{-\infty}^{\infty}\frac{d\omega}{2\pi}\frac{1}{\epsilon_l\omega^{\,2} + \mu - \widetilde{s}_d(\omega)}. \tag{3.15}$$

One can solve equation (3.13) numerically, but there it is hard to obtain good accuracy at high frequencies when the cosine term oscillates strongly. We can get a better approximation analytically. We parametrize an approximate solution by:

$$\widetilde{s}_d(\omega) = s_\infty + A\mu/(\epsilon_l \omega^2 + a^2\mu), \quad (\omega \neq 0) \tag{3.16}$$

and require that it will obey the correct behavior at low and high frequencies to leading order in the strength of the disorder. There are three parameters which are determined by $\widetilde{s}_d(\omega = 0)$, $\widetilde{s}'_d(\omega = 0)$, and $\widetilde{s}_d(\omega = \infty)$. To leading order in the strength of the disorder we can substitute in eq. (3.13),

$$b_0 = \tau, \; C_0(\zeta) = \tau(1 - \exp(-|\zeta|\sqrt{\mu/\epsilon_l}\,), \tag{3.17}$$

with $\tau = T\,/\sqrt{\epsilon_l\,\mu}$. We then find after some algebra

$$\begin{aligned} s_\infty &= \frac{4}{\mu}\widehat{f}_c\,''(\tau)(1 + \frac{1}{4}\int_0^\infty d\zeta\; e^{-\zeta}(\frac{1}{1-\alpha e^{-\zeta}} + \frac{1}{(1-\alpha e^{-\zeta})^2})) \\ &= \frac{1}{\mu}\widehat{f}_c\,''(\tau)(4 + f_1(\alpha)), \end{aligned} \tag{3.18}$$

where we defined

$$\alpha = \tau\,/(\xi^2 + \tau), \tag{3.19}$$

$$f_1(\alpha) = 1/(1-\alpha) - (1/\alpha)\log(1-\alpha). \tag{3.20}$$

Similarly for small ω we find:

$$\begin{aligned} s_d(\omega) &= \frac{4}{\mu}\widehat{f}_c\,''(\tau)(1 + \omega^2\frac{1}{8}\frac{\epsilon_l}{\mu}\int_0^\infty d\zeta\;\zeta^2 e^{-\zeta}(\frac{1}{1-\alpha e^{-\zeta}} + \frac{1}{(1-\alpha e^{-\zeta})^2}) + \ldots) \\ &= \frac{4}{\mu}\widehat{f}_c\,''(\tau)(1 + \omega^2\frac{1}{4}\frac{\epsilon_l}{\mu}f_2(\alpha) + \ldots), \end{aligned} \tag{3.21}$$

with

$$f_2(\alpha) = \frac{1}{\alpha}\sum_{k=1}^{\infty}\frac{k+1}{k^3}\alpha^k. \tag{3.22}$$

From this equation we find for the other two parameters in eq. (3.16)

$$a^2 = f_1(\alpha)/f_2(\alpha), \tag{3.23}$$

$$A = -\frac{\widehat{f_c}\,''(\tau)}{\mu}\frac{f_1^2(\alpha)}{f_2(\alpha)}. \tag{3.24}$$

Notice that $s_d(\omega)$ is negative for all $\omega > 0$. It interpolates from the value $-4|\,\widehat{f_c}\,''(\tau)|\,/\mu$ at $\omega \sim 0$ to the value $-(4 + f_1(\alpha))|\,\widehat{f_c}\,''(\tau)|\,/\mu$ at $\omega = \infty$. Substituting (3.16) in eq. (3.14) and expanding the denominator to leading order in the strength of the disorder, we get :

$$\begin{aligned} u_0^2(\ell) = C_0(\ell) = \tau(1 - A/(a^2-1)^2/\mu) \\ \times(1 - e^{-\ell/\ell^*}) + \tau A/(a(a^2-1)^2\mu) \times \\ (1 - e^{-a\ell/\ell^*}) + \tau/(2\mu) \times\ (s_\infty + A/(a^2-1)) \\ \times\ (1 - e^{-\ell/\ell^*} - (\ell/\ell^*)\ e^{-\ell/\ell^*}). \end{aligned} \tag{3.25}$$

Recall that this result is valid to first order in the strength of the columnar disorder.

This expression simplifies significantly under the assumption

$$\widetilde{B} \ll (\gamma\widetilde{T})^2, \tag{3.26}$$

valid in the experiments. In that case

$$\alpha \simeq 1 - \sqrt{\widetilde{B}}\,/\,\gamma\widetilde{T} + \cdots, \tag{3.27}$$

$$a^2 \simeq 0.351\gamma\widetilde{T}\,/\,\sqrt{\widetilde{B}} - 0.475\ \log(\sqrt{\widetilde{B}}\,/\,\gamma\widetilde{T}) + 0.326 + \cdots, \tag{3.28}$$

$$A/\mu \simeq 0.351\frac{g}{2\pi}\frac{1}{\widetilde{B}^{3/2}(\gamma\widetilde{T}\ )}(1 - (1.07 + 2.351\log(\sqrt{\widetilde{B}}\,/\,\gamma\widetilde{T}))\sqrt{\widetilde{B}}\,/\,\gamma\widetilde{T}) + \cdots, \tag{3.29}$$

$$s_\infty/\mu = -\frac{g}{2\pi}\frac{1}{\widetilde{B}\ (\gamma\widetilde{T}\ )^2}(1 + (2 - \log(\sqrt{\widetilde{B}}\,/\,\gamma\widetilde{T}))\sqrt{\widetilde{B}}\,/\,\gamma\widetilde{T}) + \cdots, \tag{3.30}$$

from which we find:

$$u^2(T)\ /\ a_0^2 \simeq 0.632\sqrt{\widetilde{B}}\gamma\widetilde{T}\ - 1.952\left(\frac{g}{2\pi}\right)\frac{1}{(\gamma\widetilde{T})^2} + 4.804\left(\frac{g}{2\pi}\right)\frac{\widetilde{B}^{1/4}}{(\gamma\widetilde{T}\ )^{5/2}} + \cdots\ . \tag{3.31}$$

From this equation we can derive the most important result for the location of the melting transition:

$$\widetilde{B}_m(\widetilde{T}) = \frac{2.504c_L^4}{(\gamma\widetilde{T})^2}\left(1 + 3.904c_L^{-2}\left(\frac{g}{2\pi}\right)\frac{1}{(\gamma\widetilde{T})^2}(1 - \frac{3.093c_L}{\gamma\widetilde{T}})\right). \tag{3.32}$$

In Fig. 1 shows a plot of $\sqrt{u^2(T)}/a_0$ vs. T for $g/2\pi = 0.025$ (curve d). We have chosen $B = 250G$. We see that the disorder tends to align the flux lines along the columnar defects, hence decreasing $u^2(T)$. Technically this happens since $\widetilde{s}_d(\omega)$ is negative.

For the case of combined columnar and point disorder, it is tempting to combine equations (2.25) and (3.32) into a single equation for $T > T_{cp}$:

$$\widetilde{B}_m(\widetilde{T}) = \frac{2.504 c_L^4}{(\gamma\widetilde{T})^2} \frac{1 + 3.904 c_L^{-2}\left(\frac{g}{2\pi}\right)\frac{1}{(\gamma\widetilde{T})^2}(1 - \frac{3.093 c_L}{\gamma\widetilde{T}})}{\left(1 + 0.209\left(\frac{\gamma\widetilde{\Delta}}{2\pi}\right)\frac{1}{(\gamma\widetilde{T})^3}\right)^2}. \tag{3.33}$$

Even the naturally grown crystals has some amount of point disorder as discussed above.

In Fig. 2 we show the modified melting line $B_m(T)$ in the presence of columnar disorder and a small amount of point disorder ($\widetilde{\Delta}/2\pi = 0.144$, corresponding to the 'as grown' curve fit of the last section), as given by eq. (3.33) with $c_L = 0.162$. We see that the melting line shifts towards higher magnetic fields with increasing amounts of columnar disorder. The best fit to the experimental results is obtained for $g/2\pi = 0.01$ and $g/2\pi = 0.025$ respectively.

For $T < T_c \approx (\epsilon_0\xi/\gamma)[4g^2\Phi_0\ /\ (\pi^2\xi^2 B)]^{1/6}$, there is a solution with RSB. This temperature is below the bottom of the range plotted in the figures for columnar disorder. It is thus not necessary to include the RSB solution in the plot.

IV. CONCLUSIONS

The analytical expressions given in eqs. (2.25), (3.32), though quite simple, seem to capture the essential feature required to reproduce the position of the melting line. The qualitative agreement with experimental results is remarkable, especially the opposite effects of point and columnar disorder on the position of the melting line. The 'as grown' experimental results are, as expected, corresponding to small amount of point disorder.

The effect of point disorder is to increase the transverse excursions of the FL which seeking the best free-energetic configuration. This increase in the mean square fluctuations lowers the melting temperature for a given magnetic field. At low temperature, the entanglement transition is associated in our formalism with RSB, and is a sort of a spin-glass

transition in the sense that many minima of the random potential and hence free energy, compete with each other. This means that there are many possible deformations of the FL which are very close in energy, or free energy. To our knowledge this is the first time the transition into the vortex glass is represented as a RSB transition.

For point disorder, in the limit of infinite cage ($\mu \to 0$), the variational approximation gives a wandering exponent of 1/2 for a random potential with short ranged correlations [11], whereas simulations give a value of 5/8 [12]. This discrepancy does not seem of importance with respect to the conclusions obtained in this paper since we always consider the case of finite μ (which amount to a non-zero magnetic field) and also consider distances of order ℓ^* in the z-direction.

For columnar disorder, the z-independence of the random potential tends to reduce the transverse fluctuations of the FL, thus shifting the melting transition to higher temperatures and magnetic fields. Related to this point is the fact that columnar disorder is much more effective in shifting the position of the melting line as compared with point disorder for the range of parameters considered here. We have used a much weaker value of correlated disorder to achieve a similar or even larger shift of the melting line than for the case of point disorder. This is again related to the z-independence of the random potential in the columnar case, which help to enhance its effect on the excursions of the vortex lines.

The experiments show that in the case of columnar disorder the transition into the vortex glass seems to be absent. In our model it corresponds to the fact that RSB does not occur in the temperature range of relevance to the experiments, but rather at significantly lower temperatures for the amount of disorder present.

Concerning the apparent deviations of the theoretical curves from the experimental points at high temperatures, we should point out that our expressions are only valid far from Tc which is $\simeq$90K for BSCCO. Close to T_c the melting line cannot behave as $B_m \propto 1/T^2$ since it must terminate at B=0, $T = T_c$. This comes about because of the temperature dependence of the fundamental constants like the penetration and coherence lengths. Houghton *et al.* [13] used a detailed melting theory to obtain a behavior of $B_m \approx B_0(1 - T/T_c)^2$ near Tc.

Other authors [14]predict a behavior like $B_m \approx B_0(T_c/T - 1)$, which seems to better fit the experimental data for the system under consideration according to ref. [6]. Adding such a correction factor to our expression for $B_m(T)$ can improve the fit at high temperatures.

Another point we should mention is that our model incorporates the disorder as depending on a single parameter like $\widetilde{\Delta}$ or g , whereas experimentally there are two parameters which are the density of defects, which is varied experimentally, and their individual strength over which there is not much control. Our model is valid in the limit of very weak impurities which are densely and uniformly distributed in space. This is quite reasonable for the case of point disorder, but for columnar disorder the experiments involve a rather low density of columnar defects which is smaller than the density of vortices. Thus from the point of view of a single vortex the disorder is not uniformly distributed which may account for the apparent difference in curvature between theory and experiment.

We have shown that the *cage model* together with the variational approximation reproduce the main feature of the experiments. Effects of many body interaction between vortex lines which are not taken into account by the effective cage model seem to be of secondary importance. Inclusion of such collective effects within the variational formalism remains a task for the future. These effects may be responsible for the apparent difference in curvature between the experimental and theoretical curves, for the case of columnar disorder.

We thank David Nelson and Eli Zeldov for discussions. We thank the Weizmann Institute for a Michael Visiting Professorship, during which this research has been initiated.

V. APPENDIX

In this appendix we give more details of the RSB solutions for point disorder and for columnar disorder. We use some of the results found in Appendix II of MP ([11]).Using the parametrization given in eqs.(2.29) and (2.30), we find for the free energy:

$$\frac{F}{2L} = const. + \frac{\tau}{4}\frac{1-u_c}{u_c}\Sigma\sqrt{\frac{\mu}{\mu+\Sigma}} - \frac{\tau}{2}\frac{1-u_c}{u_c}\sqrt{\mu(\mu+\Sigma)}$$

$$+\beta\frac{\Delta}{8\pi}u_c\frac{1}{\xi^2+\frac{\tau}{u_c}-\frac{1-u_c}{u_c}\tau\sqrt{\frac{\mu}{\mu+\Sigma}}}+\beta\frac{\Delta}{8\pi}(1-u_c)\frac{1}{\xi^2+\tau\sqrt{\frac{\mu}{\mu+\Sigma}}}, \tag{5.1}$$

where we defined $\Delta = \widetilde{\Delta}\epsilon_0^2\xi^3$. Stationarity with respect to Σ and u_c yields equations for these two quantities. Introducing the dimensionless quantity

$$\widetilde{\Sigma} = \Sigma\xi^2/\epsilon_0, \tag{5.2}$$

and taking the limit of small μ, these equations become:

$$\widetilde{\Sigma} = \frac{u_c}{\gamma\widetilde{T}}\frac{\gamma\widetilde{\Delta}}{2\pi}\frac{1}{(1+\gamma\widetilde{T}/\sqrt{\widetilde{\Sigma}})^2}, \tag{5.3}$$

$$\sqrt{\widetilde{\Sigma}} = \frac{u_c^2}{(\gamma\widetilde{T})^2}\frac{\gamma\widetilde{\Delta}}{2\pi}\frac{1}{(1+\gamma\widetilde{T}/\sqrt{\widetilde{\Sigma}})} \tag{5.4}$$

Solving these equations we find the solutions given in equations (2.31) and (2.32). The quantities s_0 and s_1 are given by the equations:

$$s_0 = 2\beta\frac{\Delta}{4\pi}\frac{1}{(\xi^2+\frac{\tau}{u_c}-\frac{1-u_c}{u_c}\tau\sqrt{\frac{\mu}{\mu+\Sigma}})^2}, \tag{5.5}$$

$$s_1 = 2\beta\frac{\Delta}{4\pi}\frac{1}{(\xi^2+\tau\sqrt{\frac{\mu}{\mu+\Sigma}})^2}, \tag{5.6}$$

from which equation (2.33) follows in the limit of small μ.

The mean square displacement $u_0^2(\ell)$ is given by

$$\begin{aligned} u_0^2(\ell) &= 2T\int\frac{d\omega}{2\pi}(1-\cos(\omega\ell))G_{aa}(\omega) \\ &= \frac{\tau}{u_c}(1-\exp(-\ell\sqrt{\mu/\epsilon_l})) - \frac{1-u_c}{u_c}\tau\sqrt{\frac{\mu}{\mu+\Sigma}}(1-\exp(-\ell\sqrt{(\mu+\Sigma)/\epsilon_l})) \\ &\quad + s_0\frac{\tau}{2\mu}(1-\exp(-\ell\sqrt{\mu/\epsilon_l}) - (\ell\sqrt{\mu/\epsilon_l})\exp(-\ell\sqrt{\mu/\epsilon_l})). \end{aligned} \tag{5.7}$$

From this expression we obtain eq.(2.35) for small μ.

Let us discuss briefly the case of columnar disorder. In this case we showed in ref. [9]that replica symmetry is broken in a region of the $T-\hbar^2/m$ phase diagram. In the present paper we use the mapping given by equation (3.2), and in addition we take the limit $L\to\infty$. For the case of short ranged correlation of the potential a 1-step RSB has been found. In

the limit $L \to \infty$ we find that the breaking point u_c of the one step solution scales as L^{-1}. Nevertheless there is a finite contribution to observable quantities as will be discussed below. Putting

$$\widetilde{s}(z) = \begin{cases} \widetilde{s}_0 & u < u_c \\ \widetilde{s}_1 & u > u_c \end{cases} \tag{5.8}$$

$$\Sigma = u_c(\widetilde{s}_1 - \widetilde{s}_0), \tag{5.9}$$

$$u_c = y_c/L, \tag{5.10}$$

we find the following equation for the limit of large L:

$$\widetilde{s}_0/L = \frac{2}{T}\widehat{f}_c{}' \left(b_0 + \frac{2T\Sigma}{y_c\mu(\mu+\Sigma)}\right) \tag{5.11}$$

$$\widetilde{s}_1/L = \frac{2}{T}\widehat{f}_c{}' (b_0) \tag{5.12}$$

$$\begin{aligned}\widetilde{s}_d(\omega) = -\Sigma + \frac{4}{\mu+\Sigma}\widehat{f}_c{}'' (b_0) - \frac{2}{T}\int_0^\infty d\varsigma(1-\cos(\omega\varsigma)) \\ \times(\widehat{f}_c{}'(C_0(\varsigma)) - \widehat{f}_c{}'(b_0)),\end{aligned} \tag{5.13}$$

and Σ and y_c satisfying the equations

$$\Sigma = \frac{2y_c}{T}\left(\widehat{f}_c{}' (b_0) - \widehat{f}_c{}' \left(b_0 + \frac{2T\Sigma}{y_c\mu(\mu+\Sigma)}\right)\right), \tag{5.14}$$

$$\begin{aligned}0 = -T^2\Sigma + T^2(\mu+\Sigma)\log(1+\Sigma/\mu) \\ +y_c^2(\mu+\Sigma)\left(\widehat{f}_c (b_0) - \widehat{f}_c \left(b_0 + \frac{2T\Sigma}{y_c\mu(\mu+\Sigma)}\right)\right. \\ \left.+\frac{2T\Sigma y_c}{\mu}\widehat{f}_c{}' \left(b_0 + \frac{2T\Sigma}{y_c\mu(\mu+\Sigma)}\right)\right).\end{aligned} \tag{5.15}$$

These equations possess a RSB solution (they always posses the solution $\Sigma = 0$) below a temperature T_c, which for small μ is given by

$$\gamma\widetilde{T}_c = \left(\frac{2g}{\pi}\right)^{1/3}\widetilde{B}^{-1/6}. \tag{5.16}$$

Just below T_c we find to leading order in $T_c - T$:

$$\widetilde{\Sigma} \sim \frac{3}{2}\widetilde{B}\left(\frac{\widetilde{T}_c - \widetilde{T}}{\widetilde{T}_c}\right), \tag{5.17}$$

$$y_c \sim \frac{3}{\gamma\widetilde{B}^{1/2}}\left(1 - 3\frac{\widetilde{T}_c - \widetilde{T}}{\widetilde{T}_c}\right). \tag{5.18}$$

REFERENCES

[1] G. Blatter *et al.*, Rev. Mod. Phys. **66**, 1125 (1994).

[2] T. Giamarchi and P. Le Doussal, Phys. Rev. Lett. **72**, 1530 (1994); Phys. Rev. **B52**, 1242 (1995); see also T. Nattermann, Phys. Rev. Lett. **64**, 2454 (1990).

[3] E. Zeldov *et al.*, Nature **375**, 373 (1995); see also H. Pastoria *et al.* Phys. Rev. Lett. **72**, 2951 (1994).

[4] M. Feigelman, *et al.*, Phys. Rev. Lett. **63**, 2303 (1989); A. I. Larkin and V. M. Vinokur, ibid. **75**, 4666 (1995).

[5] D. S. Fisher, M. P. A. Fisher and D. A. Huse, Phys. Rev. **B43**, 130 (1990).

[6] B. Khaykovitch *et al.*, Phys. Rev. Lett. **76**, 2555 (1996) and preprint (1996).

[7] D. Ertas and D. R. Nelson, preprint, cond-mat/9607142 (1996).

[8] D. R. Nelson, Phys. Rev. Lett. **60**, 1973 (1988); D. R. Nelson and V. M. Vinokur, Phys. Rev. **B48**, 13060 (1993).

[9] Y. Y. Goldschmidt, Phys. Rev. E **53**, 343 (1996).

[10] H-Y. Chen and Y. Y. Goldschmidt, J. Phys. A: math. Gen. **30**, 1803 (1997).

[11] M. Mezard and G. Parisi, J. Phys. I (France)**1**, 809 (1991).

[12] T. Halpin-Healy and Y.-C. Zhang, Phys. Rep. **254**, 215 (1995) and references therein.

[13] A. Houghton, R. A. Pelcovits and A. Sudbo, Phys. Rev. B **40,** 6763 (1989); E. H. Brandt, Phys. Rev. Lett. **63**, 1106 (1989).

[14] L. I. Glazman and A. H. Koshelev, Phys. Rev. B **43**, 2835 (1991); L. L. Daemen et al., Phys. Rev. Lett. **70**, 1167 (1993).

Figure Captions:

Fig1: Transverse fluctuations vs. temperature in the cage model for fixed $B = 250G$. (a) no disorder (b)point disorder ($\widetilde{\Delta}/(2\pi) = 0.2$) (c)RSB for point disorder, $T < T_{cp}$, (d)columnar disorder ($g/(2\pi) = 0.025$)

Fig. 2: Melting line for different amount of point and columnar disorder. The experimental points from ref. [6] are denoted by symbols and the theoretical prediction by lines. (a) squares: as grown sample, continuous curve $\widetilde{\Delta}/(2\pi) = 0.144$. (b) circles: point disorder induced by a dose of $3 \times 10^{18} e^{-}/cm^2$, dashed line $\widetilde{\Delta}/(2\pi) = 0.208$. (c) triangles: point disorder induced by a dose of $6 \times 10^{18} e^{-}/cm^2$, dotted line $\widetilde{\Delta}/(2\pi) = 0.280$. (d) inverted triangles: columnar disorder equivalent to $B_\phi = 50G$, dashed-double-dotted line $g/(2\pi) = 0.01$ and $\widetilde{\Delta}/(2\pi) = 0.144$. (e) diamonds: columnar disorder equivalent to $B_\phi = 100G$, dashed-dotted line $g/(2\pi) = 0.025$ and $\widetilde{\Delta}/(2\pi) = 0.144$.

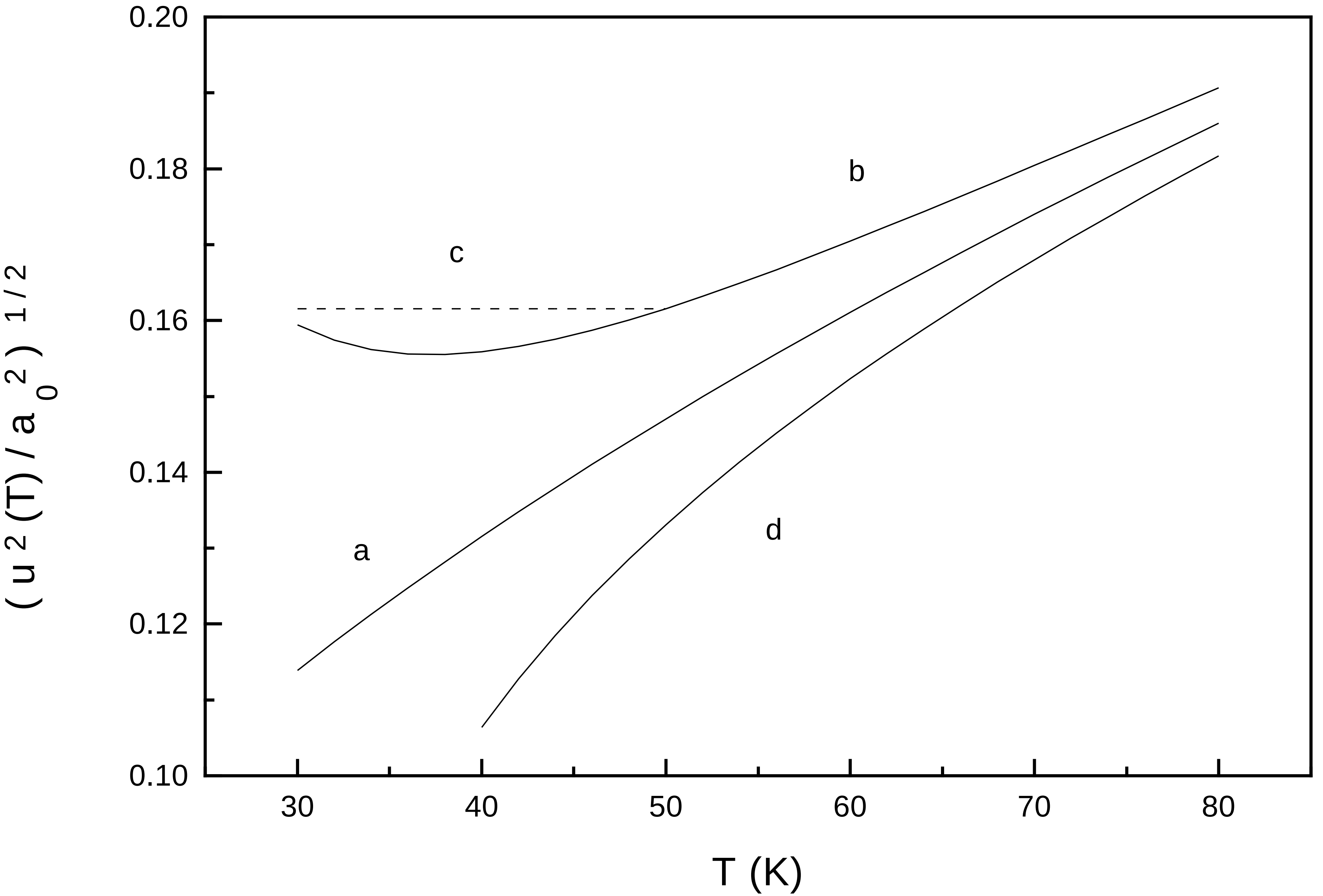

0.20
0.18
0.16
0.14
0.12
0.10
30
40
50
60
70
80
T (K)
(u 2 (T) / a 0 2) 1 / 2
a
b
c
d

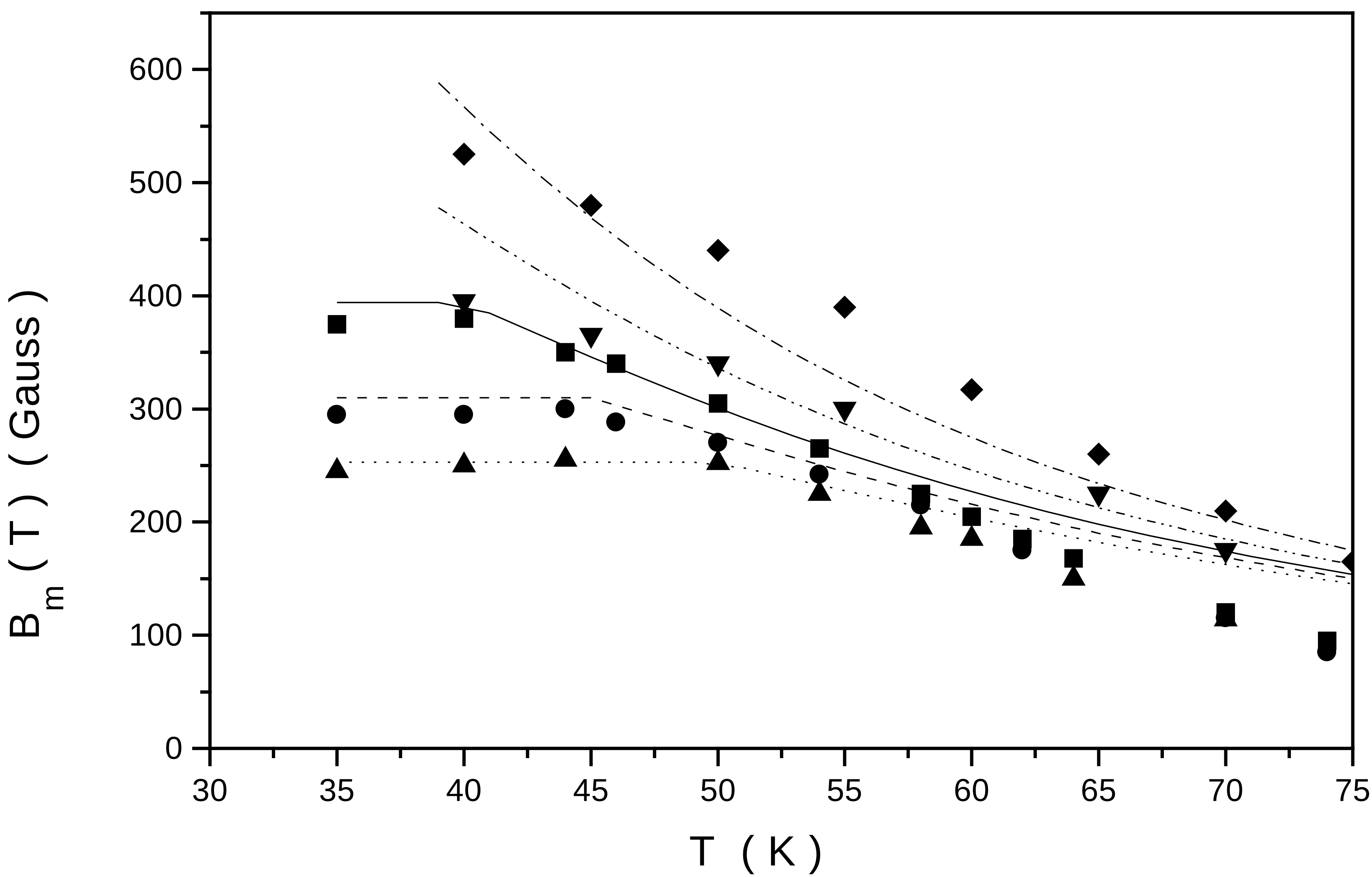

0
100
200
300
400
500
600
30
35
40
45
50
55
60
65
70
75
T (K)
B_m (T) (Gauss)